Synthesis and Assembly of Magnetite Nanocubes into Flux-Closure Rings

ARTICLE *in* THE JOURNAL OF PHYSICAL CHEMISTRY C · APRIL 2007

Impact Factor: 4.77 · DOI: 10.1021/jp070957p

Synthesis and Assembly of Magnetite Nanocubes into Flux-Closure Rings

Ying Xiong,[†,‡] Jing Ye,[†,‡] Xiaoyu Gu,[‡] and Qian-wang Chen*[,†,‡]

Division of Nanomaterials and Chemistry, Hefei National Laboratory for Physical Sciences at Microscale, University of Science and Technology of China, Hefei 230026, People's Republic of China, and Department of Materials Science and Engineering, University of Science and Technology of China, Hefei 230026, People's Republic of China

Received: February 3, 2007; In Final Form: March 29, 2007

Single-crystalline magnetite nanoparticles with a relatively narrow size distribution around 48 nm were solvothermally synthesized in a water−alcohol mixed solvent solution at 230 °C using ferrocene ($(C_5H_5)_2Fe$), polyvinylpyrrolidone (PVP), and hydrogen peroxide (H_2O_2) as starting materials. These magnetite nanoparticles exhibited almost standard cube-like shape and were coated with a thick PVP layer (∼8 nm) to form a magnetite−PVP core−shell structure. Driven by strong magnetic dipolar attractions, magnetite nanocubes could be assembled into flux-closure rings, which consisted of several to dozens of nanocubes. The rings had one-particle annular thickness, and individual nanocubes were spaced fully together. It was found that only nanocubes, the average size of which was close to 50 nm, could be assembled into rings, while slightly smaller particles were aligned in dipolar chains, suggesting that ring self-assembly could be produced by the degradation of dipolar chains that were a metastable structure with respect to rings, and only larger nanocubes with strong magnetic dipoles could overcome the potential barrier for the transformation from chains to rings.

Introduction

From both a fundamental and a technological point of view, nanocrystals with controlled shape are of crucial importance because of the strong shape-dependence of their chemical and physical properties.[1−3] For magnetic nanomaterials, the effect of shape on magnetic properties is of special prominence due to the presence of shape anisotropy. Up to now, a wealth of methods has been developed for the synthesis of magnetic nanostructures with well-controlled shape, including nanowires,[4] nanotubes,[5] nanocables,[6] nanobelts,[7] and nanoflowers.[8] Recently, magnetic nanocubes, the ideal building blocks for the formation of two-dimensional (2D) or 3D nanocrystal superlattices, have attracted intensive interest. Iron, cobalt, and iron-based alloy nanocubes have been synthesized by thermal decomposition of relevant organometallic compounds.[9−11] Urban and co-workers have reported a hydrothermal synthesis of single-crystalline $La_{1-x}Ba_xMnO_3$ nanocubes with a different x value.[12]

Magnetite (Fe_3O_4) nanocrystals have been widely investigated over the past decade due to the interesting fundamental understanding of nanomagnetism[13−15] and the promising applications in magnetic data storage,[16,17] ferrofluid,[18] sensors,[19] spintronics,[14,15] and especially biomedical fields.[20−22] However, there are no reports on the chemical synthesis of well-crystallized magnetite nanoparticles with regular cubic structure.

Dipole-directed assembly of magnetic nanoparticles into ordered structures is also intriguing. As depicted in many theoretical simulations and experimental studies, these ordered structures are expected only when the dipolar−dipolar interaction that has a strong volume dependence tends to be dominant.[23−25] Therefore, the development of a facile method for the preparation of larger magnetite nanoparticles (d > 40 nm) with a relatively narrow size distribution is an urgent task for harvesting various dipolar structures and understanding fundamental physical chemistry of dipolar ferrofluid.[26] However, the simple process toward these magnetite nanoparticles has had only limited success.[27]

Magnetic nanoparticle rings, a unique dipolar ordered structure, have been proposed as elements in novel device architecture for vertical magnetoresistive random-access memory (MRAM).[28] The magnetic dipoles in such rings are aligned into a closed circuit, and their magnetostatic fields can be entrained into chiral domains commonly referred to as flux-closure (FC) states, which have net zero-moment and minimum magnetic energy outside of the ring.[29,30] Until now, only a little work has been involved in the formation of flux-closure nanoparticle rings.[30−32] For example, Tripp and co-workers have reported that surfactant-stabilized cobalt nanoparticles can self-assemble into flux-closure rings induced by dipole interaction.[30,31] Although the flux-closure nanoparticle rings of Fe_3O_4 were first observed by Philipse et al., complicated processes including bacterial cultivation, magnetite preparation, extraction, and purification were necessarily employed, and the yield of nanoparticle rings was very low.[32]

Herein, we describe a facile solvothermal oxidization approach for the direct preparation of single-crystalline magnetite nanocubes with large size (∼48 nm) and a relatively narrow size distribution in the presence of polyvinylpyrrolidone (PVP). The possible mechanism and the appropriate conditions for assembling these nanocubes into flux-closure rings were investigated.

* To whom correspondence should be addressed. E-mail: cqw@ustc.edu.cn. Telephone: (+86)551-360-7292. Fax: (+86)551-360-7292.

† Division of Nanomaterials and Chemistry.

‡ Department of Materials Science and Engineering.

10.1021/jp070957p CCC: $37.00
Published on Web 04/20/2007

Experimental Section

Materials. Ferrocene ($(\eta$-$C_5H_5)_2Fe$, ≥98%), polyvinylpyrrolidone (PVP, K30), hydrogen peroxide (H_2O_2, 30%), and alcohol (≥99%) were purchased from Sinopharm Chem Reagent Co. All chemicals were of analytic grade (AR) and used as received without further purification.

Synthesis of Magnetite Nanoparticles. In a typical synthesis, 1.0 g of ferrocene and 5.0 g of PVP were dissolved in a mixed solution of distilled water (32.0 mL) and alcohol (8.0 mL). After sonication for 15 min (250 W ultrasonic power), the mixture solution was vigorously stirred for 15 min with a magnetic stirring apparatus. Then, 1.0 mL of hydrogen peroxide was slowly added into the above mixture solution. After that, the precursor solution was transferred to the Teflon-lined stainless autoclave with the total volume of 50.0 mL, which was put in an oven at 230 °C for 24 h and then naturally cooled to room temperature. The black products were collected by applying a cylindrical self-made permanent NdFeB magnet (~0.23 T, Φ 50 mm × 12 mm), and the supernatant was discarded by decantation. The precipitates were then washed by alcohol four times to remove excess ferrocene and PVP. Finally, the black products were dried at room temperature in a vacuum oven.

Characterization. X-ray powder diffraction (XRD) patterns were collected on a Japan Rigaku D/max-γA X-ray diffractometer using graphite-monochromatized high-intensity Cu Kα radiation (λ = 1.54178 Å). Transmission electron microscopy (TEM) images were taken on a Hitachi Model H-800 instrument with a tungsten filament, using an accelerating voltage of 200 kV. High-resolution transmission electron microscopy (HRTEM) images and electron diffraction (ED) patterns were recorded with a JEOL-2010 transmission electron microscope operating at 200 kV. Field emission scanning electron microscopy (FE-SEM) images were carried out on a JEOL JSM-6700M scanning electron microscope. The Raman spectrum was taken on a LABRAM-HR Confocal Laser Micro-Raman spectrometer using an Ar^+ laser with 514.5 nm at room temperature. The FT-IR spectrum was obtained using a Magna-IR 750 spectrometer in the range of 400−4000 cm^{-1} with a resolution of 4 cm^{-1}. Thermogravimetric (TG) analysis was performed on a Perkin-Elmer Diamond TG/DTA with a heating rate of 10 °C/min in air. Magnetic studies were carried out with a vibrating sample magnetometer on a physical properties measurement system (PPMS) at room temperature.

Results and Discussion

Structure Characterization. A typical X-ray diffraction (XRD) pattern of the as-prepared black products is shown in Figure 1a. All of the reflection peaks can be well assigned to a spinel structure with the characteristic reflections of iron oxide (γ-Fe_2O_3, JCPDS file 39-1346, or Fe_3O_4, JCPDS file 19-0629). No other impurities such as α-Fe_2O_3, $Fe(OH)_3$, and FeOOH can be observed. However, it is well-known that the clear identification of γ-Fe_2O_3 and Fe_3O_4 based on the ordinary XRD pattern is an arduous work due to the same spinel structure and the similar lattice parameter *a* (0.8346 nm for γ-Fe_2O_3 and 0.8396 nm for Fe_3O_4).[33] To clarify the phase of the as-prepared products clearly, further characterizations should be carried out to obtain more convincing evidence.

Recent works have suggested that a Raman spectrum is a simple and direct tool to differentiate the iron oxide phase, especially γ-Fe_2O_3 and Fe_3O_4.[27,34,35] A representative Raman spectrum of the as-prepared products is presented in Figure 1b. It exhibits two clear peaks at 665 and 540 cm^{-1}, which can be indexed in the A_{1g} and T_{2g} transitions of magnetite, respectively.[35,36] No characteristic bands of maghemite (720, 500, and 350 cm^{-1}) or hematite (390, 280, and 220 cm^{-1}) were observed, indicating the black products can be ascribed as a pure magnetite phase.

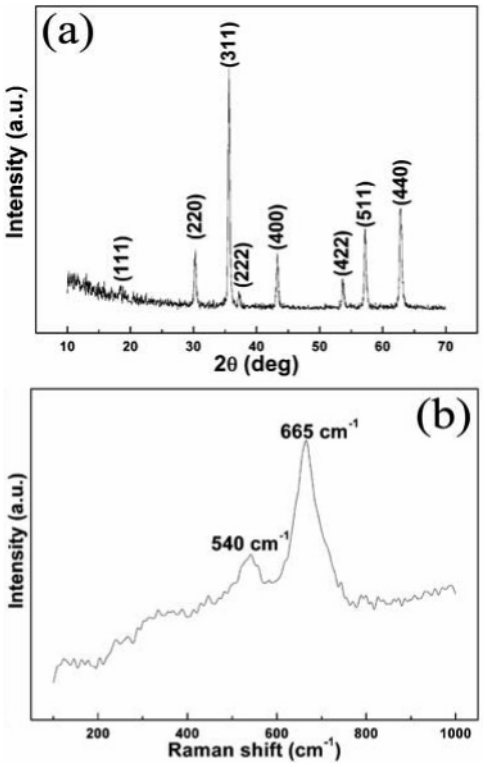

Figure 1. (a) XRD pattern and (b) Raman spectrum of the as-prepared products.

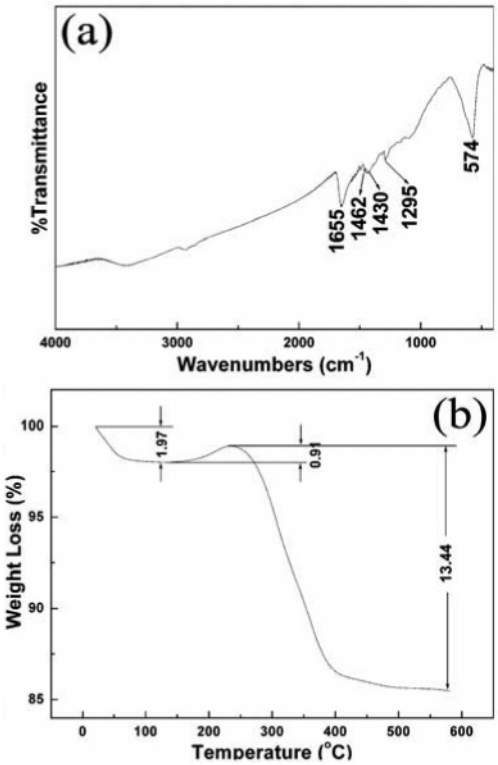

Figure 2. (a) FT-IR spectrum and (b) TG curve of the as-prepared products.

Figure 2a shows a FT-IR spectrum of the as-obtained products. The strong peak at 574 cm^{-1}, assignable to the Fe−O stretching mode of the tetrahedral and octahedral sites, can be

obviously found. Nasrazadani and co-workers have suggested that magnetite usually exhibits two strong bands at 570 and 390 cm^{-1}, and the absorbing peaks of maghemite appear at 630 and 430 cm^{-1}.[37] Therefore, the FT-IR result also reveals that the phase of the as-prepared products is magnetite rather than maghemite. The bands around 1462 and 1430 cm^{-1} may be attributed to the bond absorption of pyrrolidinyl ($-C_4H_8N$), and the band at 1295 cm^{-1} is due to the bond vibrations of the N→H−O complex, similar to the values of free PVP molecules.[38] This result indicates the presence of PVP molecules in the products. Moreover, it is notable that the stretching band of C═O at 1664 cm^{-1} for pure PVP is shifted to 1655 cm^{-1} for the as-obtained products, which suggests that PVP molecules could be adsorbed on the surface of magnetite particles by chemical bonding.[39] To determine the actual amount of PVP adsorbed on the magnetite particles, TG analysis was performed on the dried samples in air. Figure 2b is a TG curve of the as-obtained products. The first and brief event of weight loss (1.97%) that occurred below 100 °C is due to the dehydration of the power. A weight gain effect (0.91%) between 154 and 235 °C is attributed to the transformation of magnetite into maghemite.[35a] The main weight loss (13.44%) in the range of 235−570 °C can be ascribed to the slow decomposition of PVP. Therefore, we could roughly estimate that the percentage of magnetite particles in the products is about 85%.

Morphology Characterization. The shape of the magnetite particles was characterized by SEM and TEM. Figure 3a and b shows representative SEM and TEM images of the as-prepared magnetite particles, respectively. From each figure, it can be seen that these particles have a relatively narrow size distribution and uniform shape, respectively. Interestingly, the SEM image (Figure 3a) reveals that the as-synthesized magnetite has a sphere-like shape with the average size of 68 ± 10 nm, but the cube-like morphology of the as-synthesized magnetite with the average size of 48 ± 8 nm can be observed in the TEM image (Figure 3b). Combined with the previous results of FT-IR and TG, two obvious differences in shape and size strongly suggest that the magnetite nanoparticles have a magnetite−PVP core−shell structure. To accurately confirm the morphology of these magnetite nanoparticles, tilted TEM investigation was performed to obtain the transmission images from different viewing angles (Φ). Figure 3c presents a TEM image of the nanoparticles prior to tilting (Φ = 0°), which reveals that magnetite nanoparticles have an almost standard square shape and clear-cut edges. After the sample (the copper grid) was tilted with an angle of Φ = 30°, it was observed (in Figure 3d) that the shape of the nanoparticles are elongated and transformed from square to hexagon. All of these observations rationally suggest that the as-synthesized magnetite nanoparticles are indeed cube-like. Furthermore, in order to further determine their structure characteristic, we obtained a HRTEM image and ED pattern of an individual magnetite nanocube. The clear 2D lattice fringes (Figure 3f) and sharp diffraction spot (Figure 3g) reveal the single-crystalline nature of the magnetite nanocube. The distance between the adjacent lattice fringes is 0.495 nm, which is very close to the interplanar distance of fcc magnetite {111}. The ED pattern confirms that the incident electron beam is a [0−11] projection, the optimum orientation for imaging cubic-structured materials,[40] which may be the reason that the projected shape of a nanocube in a HRTEM image (Figure 3e) is a symmetric hexagon. Moreover, a thick PVP layer with ca. 8 nm (marked in Figure 3e) can be seen, directly demonstrating the magnetite−PVP core−shell structure.

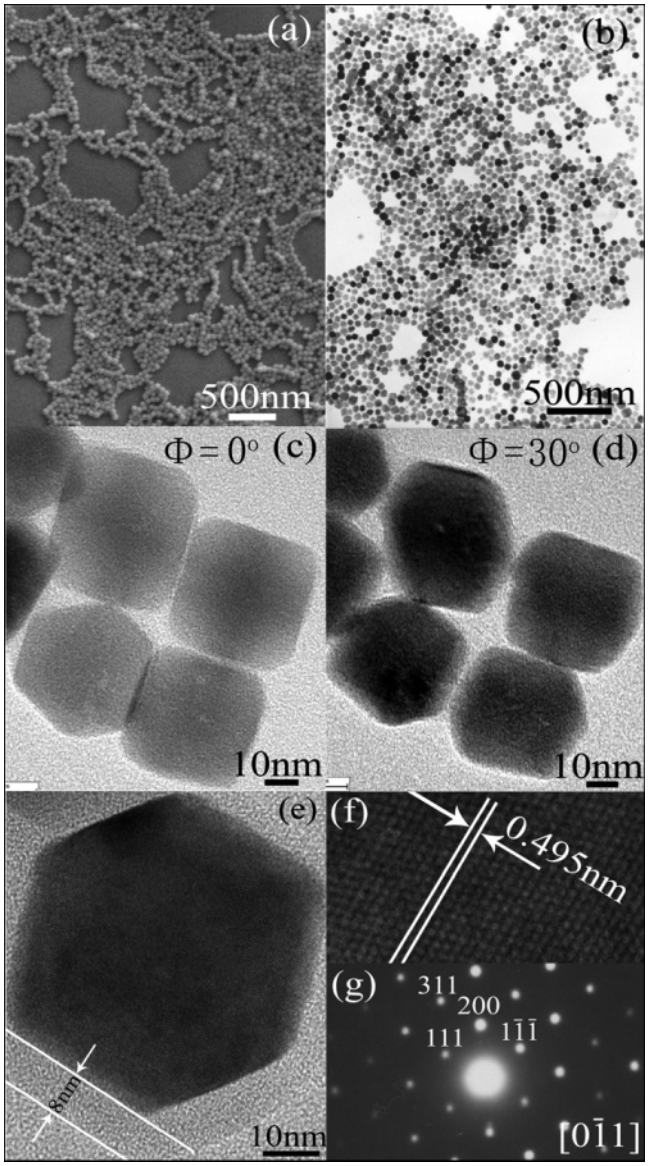

Figure 3. (a) and (b) SEM and TEM images of magnetite nanoparticles; (c) and (d) TEM images of four nanoparticles (Φ is the angle over which the copper grid is titled); (e) HRTEM images of an individual magnetite nanocube; (f) and (g) lattice fringe and electron diffraction (ED) pattern of magnetite nanocubes recorded from (e).

Assembly of Magnetite Nanoparticles into Flux-Closure Rings. This magnetite−PVP core−shell structure with excellent dispersibility in polar solvents provides an ideal system to investigate their dipole-directed assembly behavior because the PVP shell can minimize the effect of van der Waals attractions and completely screen the electrostatic interactions. To directly image the dipolar assemblies by the conventional TEM, a colloidal solution of magnetite nanocubes was cast and dried onto carbon-coated TEM grids by a standardized procedure.[31] Figure 4a shows a typical TEM image of magnetite nanocubes dispersed in ethanol when deposited in this manner. A large amount of nanocube rings (labeled as 2) can coexist with a small quantity of short dipolar chains (labeled as 1). A magnified TEM image (Figure 4b) reveals that the rings have one-particle annular thickness, and individual nanocubes are spaced fully together (this is actually the flux-closure ring predicted by Jacobs and Bean[29]). Generally speaking, nanoparticle rings can be formed by two different mechanisms, dipole-directed assembly and drying-mediated assembly.[31] The rings formed by the latter

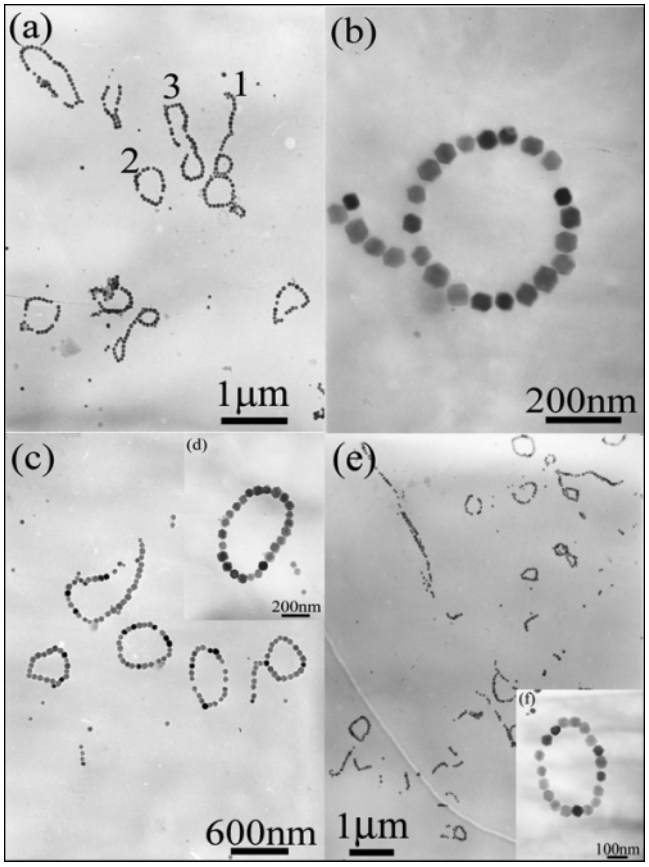

Figure 4. TEM images of magnetite nanocubes dispersed in different solvents, which have different vapor pressure; (a) and (b) ethanol (43.87 mmHg, 20 °C), (c) and (d) butanol (4.16 mmHg, 20 °C), (e) and (f) methanol (97.48 mmHg, 20 °C).

usually had a several-particles-thick wall, and individual particles were not spaced together.[41] To further clarify the actual mechanism in this study, several solvents with different vapor pressures at 20 °C were selected to disperse the magnetite nanocubes.[42] As illustrated in Figure 4, similar one-particle-thick rings can be found in all solvents, indicating that drying-mediated assembly is not responsible for the formation of these nanocube rings.

Strong dipolar−dipolar attractions between magnetic dipoles could undoubtedly induce the formation of an anisotropic chain-like structure,[25,28] but it was metastable from an energetic point of view due to the "unsaturated" end dipoles. As predicted in theoretical calculations, a closed ring in which all dipoles could be located in a circuit had the lowest energy; however, little direct evidence of the existence of nanoparticle rings among many experimental studies has been reported.[31,32,43,44] The existence of some unclosed rings in Figure 4a could provide some helpful insights about these ring self-assemblies. On the basis of the results in the TEM images, combined with the theoretical predictions by Philipse et al.,[32] the nanocube rings could be produced by the degradation of dipolar chains in the following two manners: self-closing of a single chain (labeled as 3) or interattracting between unpaired end dipoles of two or several chains (labeled as 2).

However, how could the chains degrade into the rings? In order to explain this question, magnetite nanocubes with a broad particle size distribution (∼10−60 nm) were synthesized through varying experimental parameters (not shown). Figure 5 displays the TEM images of the deposition of a colloidal solution of these magnetite nanocubes, which reveal that short chains as

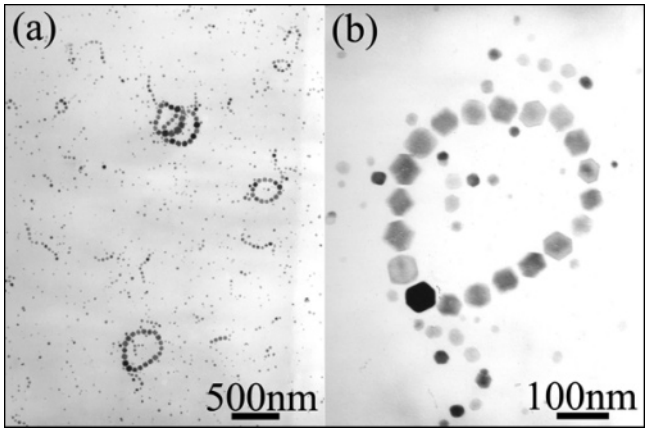

Figure 5. TEM images of the deposition of a colloidal solution of magnetite nanocubes with large differences in size.

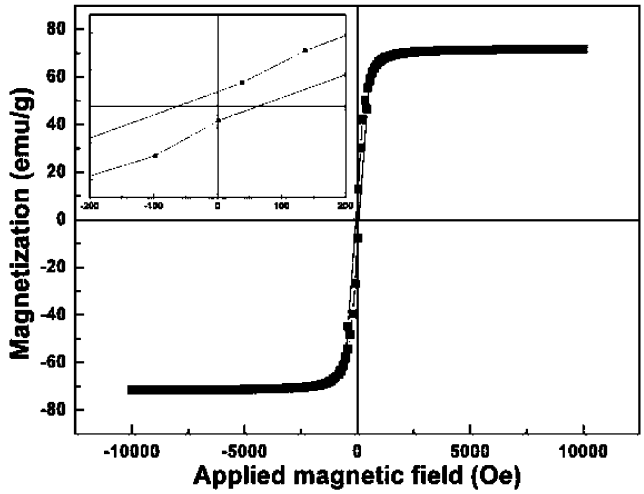

Figure 6. Field dependence of magnetization for the dried magnetite nanocubes measured at 300 K. The inset is an expanded low-field curve.

well as closed rings can coexist with many discrete nanocubes. It is notable that the cube size in the three structures is distinctly different, and the average particle size in the nanocube rings (∼50 nm) is the largest; however, that for the discrete nanocubes (∼20 nm) is the smallest. These phenomena indicated that a critical particle size was necessary for forming dipolar structures, and only large nanocubes could be assembled into closed rings.

The dipolar−dipolar interactions between two magnetic particles scale as r^6/σ^3 (r being the particle radius; σ consisting of the particle diameter and the thickness of the nonmagnetic layer).[45] For small particles, the dipolar interactions were weaker than the repulsions by the PVP shell so that they stayed discrete. As the size was in excess of a critical value, anisotropic dipolar interactions could drive the formation of chains, a simple dipolar structure. Commonly, larger nanocubes can be aligned more easily into dipolar chains, owing to stronger dipolar attractions. However, it is surprising in Figure 5 that the chains consisting of larger nanocubes could not be found and that the size of all of the chains was clearly lower than that of rings. Therefore, it could be rationally concluded that only the chains consisting of larger nanocubes could be transformed into closed rings that possessed lower energy, while slightly smaller cubes were just aligned into chains, indicating the existence of a potential barrier for the transformation from chains to rings. That is to say, only larger nanocubes with stronger magnetic dipoles could overcome the potential barrier, which could involve an energetic cost for

bending chains and an entropic cost of constraining unpaired end dipoles of chains to the same region.[26] These results also suggest that dipole-ordered structures formed by dipole-directed assembly have a strong size dependence.

Moreover, the other puzzling question is why the chains but not the rings were usually obtained in many previous studies, that is to say, does the cube-like shape of the magnetite particles favor the formation of flux-closure rings? As depicted in previous works, the unique cubic shape would possibly introduce directional, anisotropic interactions between dipoles because the dipole could orient in several directions relative to a cube face, and the strength could also vary with the orientation.[46] Recently, Zhang and co-workers[47] have studied the dipolar-induced self-assembly of nanocubes through computer simulation. They found that the ring-like structure could be obtained as some dipoles with different orientation and strength were mixed. Therefore, the formation of flux-closure rings in our system could be tentatively attributed to the unique shape of the magnetite nanocubes. More careful characterizations, such as electron holography and magnetic force microscopy, need to be carried out in a single flux-closure ring.

Magnetic Properties. The field dependence of magnetization for the magnetite nanocubes measured at 300 K is illustrated in Figure 6. From the plots of *M* versus *H*, the saturation magnetization (*M*s) of the sample is 71.7 emu/g. Considering the actual weight percentage of magnetite nanocubes in the sample (about 85%), the *M*s value of pure magnetite nanocubes reaches 84.4 emu/g. Although it is slightly lower than the theoretical value of the bulk magnetite (∼92 emu/g),[48] it is obviously higher than that of similarly sized magnetite nanoparticles prepared by the other method,[49] which indicates the high crystallinity of the as-prepared magnetite nanocubes.[50] The inset of Figure 6 shows an expanded low-field hysteresis curve, which somewhat reveals ferromagnetic behavior, with the coercivity (*H*c) of 62 Oe and the reduced magnetization (*M*r/*M*s) of 0.09. Low *H*c and *M*r/*M*s values could be possibly related to the low magnetocrystalline anisotropy[13a] and/or the small particle size [the size of most of nanocubes was lower than the critical size of the single domain for magnetite (54 nm)[51]]. Furthermore, the investigation of the magnetic properties for these flux-closure rings is still in progress.

Conclusions

A facile sovlothermal approach has been reported for the preparation of single-crystalline magnetite nanoparticles with an average size of 48 nm under the assistance of PVP. The as-prepared magnetite nanoparticles had almost standard cube-like morphology and a relatively narrow size distribution. Owing to strong dipolar−dipolar attractions, magnetite nanocubes could be assembled into flux-closure rings with one-particle annular thickness through the degradation of dipolar chains, which was a stable dipolar structure with a low energy with respect to the anisotropic chains. However, there was a potential barrier for the transformation from chains to rings, and only nanocubes with a large size (∼50 nm) could overcome it. Using dipole-directed assembly to form flux-closure magnetite nanocube rings provides a way to investigate the fundamental physical properties and potential applications such as ultradense information storage.

Acknowledgment. This work is supported by the National Natural Science Foundation of China (NSFC) under Grant No. 20125103 and 90206034.

References and Notes

(1) Peng, X.; Manno, L.; Wang, W.; Wickham, J.; Scher, E.; Kadavanich, A.; Alivisatos, A. P. *Nature* **2000**, *404*, 59.
(2) O'Handley, R. C. *Mordern Magnetic Materials*; Wiley: New York, 1999.
(3) Park, J.; Lee, E.; Hwang, N. M.; Kang, M.; Kim, S. C.; Hwang, Y.; Park, J. G.; Noh, H. J.; Kim, J. Y.; Park, J. H.; Hyeon, T. W. *Angew. Chem., Int. Ed.* **2005**, *44*, 2.
(4) Wang, J.; Chen, Q. W.; Zeng, C.; Hou, B. Y. *Adv. Mater.* **2004**, *16*, 137.
(5) (a) Liu, Z. Q.; Zhang, D. H.; Han, S.; Li, C.; Lei, B.; Lu, W. G.; Fang, J. Y.; Zhou, C. W. *J. Am. Chem. Soc.* **2005**, *127*, 6. (b) Crowley, T. A.; Zieqler, K. J.; Lyons, D. M.; Erts, D.; Olin, H.; Morris, M. A.; Holmes, J. D. *Chem. Mater.* **2003**, *15*, 3518.
(6) Daly, B.; Arnold, D. C.; Kulkarni, J. S.; Kazakova, O.; Shaw, M. T.; Nikitenko, S.; Erts, D.; Morris, M. A.; Holmes, J. D. *Small* **2006**, *2*, 1299.
(7) Morber, J. R.; Ding, Y.; Haluska, M. S.; Li, Y.; Liu, J. P.; Wang, Z. L.; Snyder, R. L. *J. Phys. Chem. B* **2006**, *110*, 21672.
(8) Zhong, L. S.; Hu, J. S.; Liang, H. P.; Cao, A. M.; Song, W. G.; Wan, L. J. *Adv. Mater.* **2006**, *18*, 2426.
(9) Dumestre, F.; Chaudret, B.; Amiens, C.; Renaud, P.; Fejes, P. *Science* **2004**, *303*, 821.
(10) Gräf, C. P.; Birringer, R.; Michels, A. *Phys. Rev. B* **2006**, *73*, 212401.
(11) Chen, M.; Kim, J.; Liu, J. P.; Fan, H. Y.; Sun, S. *J. Am. Chem. Soc.* **2006**, *128*, 7132.
(12) Urban, J. J.; Ouyang, L.; Jo, M. H.; Wang, D. S.; Park, H. K. *Nano Lett.* **2004**, *4*, 1547.
(13) (a) Song, Q.; Zhang, Z. J. *J. Phys. Chem. B* **2006**, *110*, 11205. (b) Frankamp, B. L.; Boal, A. K.; Tuominen, M. T.; Rotello, V. M. *J. Am. Chem. Soc.* **2005**, *127*, 9731.
(14) Lu, Z. L.; Zou, W. Q.; Lv, L. Y.; Liu, X. C.; Li, S. D.; Zhu, J. M.; Zhang, F. M.; Du, Y. W. *J. Phys. Chem. B* **2006**, *110*, 23817.
(15) (a) Liao, Z. M.; Li, Y. D.; Xu, J.; Zhang, J. M.; Xia, K.; Yu, D. P. *Nano Lett.* **2006**, *6*, 1087. (b) Zhang, D.; Liu, Z.; Han, S.; Li, C.; Lei, B.; Stewart, M. P.; Tour, J. M.; Zhou, C. M. *Nano Lett.* **2004**, *4*, 2151.
(16) Black, C. T.; Murray, C. B.; Sandstrom, R. L.; Sun, S. *Science* **2000**, *290*, 1131.
(17) Bate, G. In *Ferromagnetic Materials, Recording Materials*; Wohlfarth, E. D., Ed.; North-Holland: Amsterdam, The Netherlands, 1980; Vol. 2, p 381.
(18) Raj, K.; Moskowitz, B.; Casciari, R. *J. Magn. Magn. Mater.* **1995**, *149*, 174.
(19) Zeng, H.; Li, J.; Liu, J. P.; Wang, Z. L.; Sun, S. H. *Nature* **2002**, *420*, 395.
(20) Mornet, S.; Vasseur, S.; Grasset, F.; Duguet, E. *J. Mater. Chem.* **2004**, *14*, 2161.
(21) (a) Stoeva, S. I.; Huo, F. W.; Lee, J. S.; Mirkin, C. A. *J. Am. Chem. Soc.* **2005**, *127*, 15362. (b) Won, J.; Kim, M.; Yi, Y. W.; Kim, Y. H.; Jung, N.; Kim, T. K. *Science* **2005**, *309*, 121.
(22) (a) Hu, F. Q.; Wei, L.; Zhou, Z.; Ran, Y. L.; Li, Z.; Gao, M. Y. *Adv. Mater.* **2006**, *18*, 2553. (b) Brähler, M.; Georgieva, R.; Buske, N.; Müller, A.; Müller, S.; Pinkernelle, J.; Teichgräber, U.; Voigt, A.; Bäumler, H. *Nano Lett.* **2006**, *6*, 2505.
(23) (a) Chantrell, R. W.; Bradbury, A.; Popplewell, J.; Charles, S. W. *J. Phys. D: Appl. Phys.* **1980**, *13*, L119. (b) Chantrell, R. W.; Bradbury, A.; Popplewell, J.; Charles, S. W. *J. Appl. Phys.* **1982**, *53*, 2742.
(24) (a) Tlusty, T.; Safran, S. A. *Science* **2000**, *290*, 1328. (b) Tavares, J. M.; Weis, J. J. M.; de Gama, M. T. *Phys. Rev. E* **2002**, *65*, 061201.
(25) (a) Klokkenburg, M.; Vonk, C.; Claesson, E. M.; Meeldijk, J. D.; Erné, B. H.; Philipse, A. P. *J. Am. Chem. Soc.* **2004**, *126*, 16706. (b) Butter, K.; Bomans, P. H. H.; Frederik, P. M.; Vroege, G. J.; Philipse, A. P. *Nat. Mater.* **2003**, *2*, 88.
(26) Safran, S. A. *Nat. Mater.* **2003**, *2*, 71.
(27) Daou, T. J.; Pourroy, G.; Bégin-Colin, S.; Grenèche, J. M.; Ulhaq-Bouillet, C.; Legaré, P.; Bernhardt, P.; Leuvrey, C.; Rogez, G. *Chem. Mater.* **2006**, *18*, 4399.
(28) (a) Li, S. P.; Peyrade, D.; Natali, M.; Lebib, A.; Chen, Y.; Ebels, U.; Buda, L. D.; Ounadjela, K. *Phys. Rev. Lett.* **2001**, *86*, 1102. (b) Rothman, J.; Kläui, M.; Lopez-Diaz, L.; Vaz, C. A. F.; Bleloch, A.; Bland, J. A. C.; Cui, Z.; Speaks, R. *Phys. Rev. Lett.* **2001**, *86*, 1098.
(29) Jacobs, I. S.; Bean, C. P.; In *Magnetism*; Rado, G. T., Suhl, H., Eds.; Academic Press: New York, 1963; Vol. III.
(30) Tripp, S. L.; Dunin-Borkowski, R. E.; Wei, A. *Angew. Chem., Int. Ed.* **2003**, *42*, 5591.
(31) Tripp, S. L.; Pusztay, S. V.; Ribbe, A. E.; Wei, A. *J. Am. Chem. Soc.* **2002**, *124*, 7914.
(32) Philipse, A. P.; Maas, D. *Langmuir*, **2002**, *18*, 9977.
(33) Thewlis, J. *Philos. Mag.* **1931**, *12*, 1089.
(34) Pinna, N.; Grancharov, S.; Beato, P.; Bonville, P.; Antonietti, M.; Niederberger, M. *Chem. Mater.* **2005**, *17*, 3044.

(35) (a) Cornell, R. M.; Schwertmann, U. *The Iron Oxide: Structure, Properties, Reactions, Occurences and Uses*, 2nd ed.; Wiely-VCH Verlag GmbH & Co. KGaA: Weinheim, Germany, 2003. (b) De Faria, D. L. A.; Venancio Silva, S.; De Oliveira, M. T. *J. Raman Spectrosc.* **1997**, *28*, 873.
(36) Shebanova, O. N.; Lazor, P. *J. Raman Spectrosc.* **2003**, *34*, 845.
(37) Nasrazadani, S.; Raman, A. *Corros. Sci.* **1993**, *34*, 1355.
(38) Zhang, Z. T.; Zhao, B.; Hu, L. M. *J. Solid State Chem.* **1996**, *121*, 105.
(39) Lee, H. Y.; Lim, N. H.; Seo, A. J.; Yuk, S. H.; Kwak, B. K.; Khang, G.; Lee, H. B.; Cho, S. H. *J. Biomed. Mater. Res., Part B* **2006**, *79*, 142.
(40) Wang, Z. L. *J. Phys. Chem. B* **2000**, *104*, 1153.
(41) (a) Elbaum, M.; Lipson, S. G. *Phys. Rev. Lett.* **1994**, *72*, 3562. (b) Ohara, P. C.; Gelbart, W. M. *Langmuir* **1998**, *14*, 3418.
(42) The data of vapor pressure were obtained from the following website: Ohe, S. Distallition, Vapor Pressure, Vapor−Liquid Equilibria. http://www.s-ohe.com/.
(43) Shen, L.; Stachowiak, A.; Fateen, S. K.; Laibins, P. E.; Hatton, T. A. *Langmuir* **2001**, *17*, 288.
(44) Donselaar, L. D.; Frederik, P. M.; Bomans, P.; Buining, P. A.; Humbel, B. M.; Philipse, A. P. *J. Magn. Magn. Mater.* **1999**, *201*, 58.
(45) Rosensweig, R. E. *Ferrohydrodynamics;* Cambridge University Press: Cambridge, U.K., **1985**.
(46) Cho, K. S.; Talapin, D. V.; Gaschler, W.; Murray, C. B. *J. Am. Chem. Soc.* **2005**, *127*, 7140.
(47) Zhang, X.; Zhang, Z. L.; Glotzer, S. C. *J. Phys. Chem. C* **2007**, *111*, 4132.
(48) Han, D. H.; Wang, H. L.; Luo, J. *J. Magn. Magn. Mater.* **1994**, *136*, 176.
(49) Wang, L. Y.; Bao, J.; Wang, L.; Zhang, F.; Li, Y. D. *Chem.—Eur. J.* **2006**, *12*, 6341.
(50) Wu, M. Z.; Xiong, Y.; Jia, Y. S.; Niu, H. L.; Qi, H. P.; Ye, J.; Chen, Q. W. *Chem. Phys. Lett.* **2005**, *401*, 374.
(51) Li, Z.; Sun, Q.; Gao, M. Y. *Angew. Chem., Int. Ed.* **2005**, *44*, 123.